Acta Biochim Biophys Sin 2024, 56(11): 1673–1686
https://doi.org/10.3724/abbs.2024134
Advance Access Publication Date: 6 August 2024
Original Article

Original Article

SUN5, a testis-specific nuclear membrane protein, participates in recruitment and export of nuclear mRNA in spermatogenesis

Xiyi He[1,2], Yunfei Zhang[1,2], Zenghui Mao[3], Gang Liu[4], Lihua Huang[1], Xiaowen Liu[3], Yuyan Su[1,2], and Xiaowei Xing[1,5,*]

[1]Center for Experimental Medicine, Third Xiangya Hospital, Central South University, Changsha 410013, China, [2]Department of Laboratory Medicine, Third Xiangya Hospital, Central South University, Changsha 410013, China, [3]Hunan Provincial Key Laboratory of Regional Hereditary Birth Defects Prevention and Control, Changsha Hospital for Maternal & Child Health Care Affiliated to Hunan Normal University, Changsha 410007, China, [4]Institute of Reproductive and Stem Cell Engineering, School of Basic Medicine, Central South University, Changsha 410078, China, and [5]NHC Key Laboratory of Birth Defects Prevention, Zhengzhou 451163, China
*Correspondence address. Tel: +86-13975806774; E-mail: davy2222@163.com

Received 18 March 2024 Accepted 24 May 2024

Abstract

SUN5, a testis-specific gene, is associated with acephalic spermatozoa syndrome (ASS). Here, we demonstrate that SUN5 is involved in mRNA export. In *Sun5*-knockout mice (*Sun5*$^{-/-}$), poly(A)$^+$ RNA accumulates in the nuclei of germ cells, leading to reduced sperm counts, decreased sperm motility and disrupted sperm head-to-tail junctions. Additionally, in the GC-2 germ cell line with RNA interference of *Sun5*, heterogeneous nuclear ribonucleoproteins (hnRNPs) and poly (A)$^+$ RNA (mainly mRNA) are retained in the nucleus. Further mechanistic studies reveal that SUN5 interacts with Nxf1 (nuclear RNA export factor 1) and nucleoporin 93 (Nup93). Interference with Nup93 inhibits mRNA export. Treatment with leptomycin B to block the CRM1 pathway indicates that *Sun5* regulates mRNA export through an Nxf1-dependent pathway. In *Sun5*$^{-/-}$ mice, the binding of Nxf1 and Nup93 decreases due to loss of Sun5 function, and the process of submitting Nxf1-binding mRNPs to Nup93 is inhibited, resulting in abnormal spermatogenesis. Together, these data may elucidate a novel pathway for mRNA export in male germ cells.

Key words SUN5, hnRNPs, Nup93, Nxf1, mRNA export

Introduction

Spermatogenesis is a complex process in which spermatogonial stem cells undergo a series of differentiations to produce haploid spermatids, after which the spermatids develop into mature spermatozoa [1]. At each stage, testis-specific genes are involved and exert their specific functions. Genes are transcribed in the nucleus, encased in messenger ribonucleoprotein particles (mRNPs) and translocated to the cytoplasm via the nuclear pore complex (NPC) for immediate translation or storage [2,3]. However, the function and molecular mechanism of these testis-specific genes in mRNA nuclear export are still unclear.

Pre-mRNAs are packaged into mRNPs by loading with different RNA-binding proteins (RBPs). Current studies have demonstrated that in eukaryotes, certain RBPs are deposited at specific locations on pre-mRNAs when transcribed for synthesis [4]. As a large class of RBPs, heterogeneous nuclear ribonucleoproteins (hnRNPs) affect multiple aspects of mRNA metabolism, including the encasing of nascent transcripts, alternative splicing, nucleus-to-cytoplasm transport and translational regulation [5]. In humans, approximately 30 different hnRNPs (called A1 to U) bind to different transcripts synthesized by RNA-pol-II in the nucleus [6]. HnRNPs, such as hnRNP K, depart from mRNPs before being exported or rapidly shuttling back from the cytoplasm to the nucleus [7]. HnRNPs assist in the control of pre-mRNA maturation into mRNAs and accompany the mRNA at different stages [6].

RNA is transported from the nucleus to the cytoplasm in different ways and is broadly categorized into two forms: the chromosomal region maintenance 1 (CRM1) pathway and the nuclear RNA export factor 1 (NXF1) pathway, depending on the transporter receptor [8]. A small subset of mRNAs and various miscellaneous RNAs, such as

miRNAs and lncRNAs, are mainly transported by the CRM1 protein, similar to karyopherin [9]. However, the transport of most constitutively expressed mRNAs is mediated by the NXF1-NXT1 heterodimer, despite the variety of mRNAs in terms of splicing, maturation state, size, copy number, etc. [10]. NXF1 consists of four domains: a leucine-rich region (LRR), an RNA recognition motif (RRM), an NTF2-like domain (NTF2L) which binds NXT1 to form the NXF1/NXT1 heterodimer, and a ubiquitin-associated (UBA) domain [11]. In the process of mRNA export, the NXF1-NXT1 heterodimer is loaded onto mRNPs via the transcription export complex (TREX), and mRNPs with export capability are assembled in preparation for translocation [12,13].

Mature mRNPs are targeted and translocated through the NPC by fast, transient interactions with multiple phenylalanine (F)-glycine (G) repeat sequences (FG repeats) of nucleoporins [14]. According to its position, the NPC complex is divided into three parts: nucleoplasmic regions, cytoplasmic filaments and nuclear basket nucleoporins [15]. In humans, the NPC contains approximately 32 nucleoporins, almost half of which have FG repeats [16]. Previous studies have demonstrated that many nucleoporins, such as Nup153 [17], Nup62 [18], Nup155 [19], Nup188 [20] and Tpr [21], participate in mRNA transport.

Here, we demonstrated that the nuclear membrane protein SUN5, which belongs to the Sun domain protein family, is involved in mRNA export during spermatogenesis. *SUN5*, also known as *TSARG4* and *SPAG4L*, was first cloned and registered in GenBank (AF401350) by our team. In previous research, we found that *Sun5* is a testis-specific gene in mice and that its encoded protein interacts with Nesprin3 to form the linker of the nucleoskeleton and cytoskeleton (LINC) complex, which is required for sperm head-to-tail junctions [22]. Recently, we performed immunoprecipitation-mass spectrometry (IP-MS) to screen potential SUN5-interacting proteins in mouse testes and discovered that SUN5 may interact with proteins involved in mRNA export, such as hnRNPs (hnRNP K, hnRNP F/H1), Nxf1, and Nup93, indicating that *Sun5* may participate in mRNA transport, but the function and molecular mechanism involved are still unclear.

In this study, we established *Sun5*-knockout mice (*Sun5*$^{-/-}$) and *Sun5*-knockdown cell lines (GC-2 and LoVo) and observed that the mRNA aggregates in the nucleus. To further explore the function and role of SUN5, we demonstrated that *Sun5* engages in mRNA transport by interacting with Nxf1 and Nup93. This work provides new insights into the molecular mechanism of mRNA export in male germ cells.

Materials and Methods

Coimmunoprecipitation (co-IP) and mass spectrometry

The pLVX-IRES-Puro-SUN5-Flag lentivirus was obtained from Yingrun Biotechnologies, Inc. (Changsha, China), and used to transfect NTERA-2 cells, which were purchased from the American Type Culture Collection (ATCC; Manassas, USA), as described in our previous study [22]. Testicular tissues from C57BL/6J mice, or stably transfected cells ground with liquid nitrogen were lysed with 1 mL of IP lysis solution (Thermo Fisher Scientific, Waltham, USA) supplemented with a cocktail of phosphatase inhibitors (Glpbio, Montclair, USA) on ice. After being lysed for 15–30 min, the solution was centrifuged for 30 min at 4°C to separate the supernatant. The antibodies were bound to magnetic beads at 4°C for 6 ~ 8 h in advance. According to the instructions of the Co-IP Kit (Thermo Fisher Scientific), total protein was incubated with magnetic bead/antibody complexes at 4°C with rotation overnight. Then, western blot analysis was conducted on the subsequently obtained purified protein. Afterward, the polyacrylamide gel was stained with silver, and finally the gels were cut and sent to Bioprofile (Shanghai, China) for LC-MS/MS analysis. The experiments to detect the binding strength of Nxf1 and Nup93 were performed in triplicate.

Western blot analysis

Testicular tissues of mice were ground with liquid nitrogen, and the collected cells were lysed in radioimmunoprecipitation assay (RIPA) buffer (Beyotime, Shanghai, China) supplemented with protease inhibitor cocktail (Cellpro, Suzhou, China) and phenylmethanesulfonyl fluoride (PMSF) (Biosharp, Hefei, China) on ice. Then, western blotting was performed with standard procedures. Horseradish peroxidase-conjugated anti-rabbit or mouse IgG secondary antibodies (Beyotime, 1:1000) were used for hybridization for 1 h at room temperature. Signals were visualized using an enhanced chemiluminescent (ECL) kit (Biosharp, Hefei, China), photographed, and quantified with the VisionWorks system (AnalytikJena AG, Jena, Germany). The antibodies used for western blot analysis are listed in Supplementary Table S1. The results are representative of at least three independent experiments.

Immunofluorescence assay

Cell climbing sheets were prepared and then fixed in 4% paraformaldehyde at room temperature for 10 min or more. Subsequently, after permeabilization with 0.5% Triton X-100 and blocking with 5% BSA, the glass slides were hybridized with primary antibodies at 4°C overnight. The antibodies used in the immunofluorescence assay are listed in Supplementary Table S1. After 3 times wash with PBS, the cells were incubated with a fluorescent secondary antibody (Proteintech, Wuhan, China) at room temperature for 1 h. The nuclei were stained with DAPI, blocked with glycerol, and finally observed under a fluorescence microscope (Zeiss, Jena, Germany). Each process was repeated three times.

Generation of *Sun5*-knockout (*Sun5*$^{-/-}$) mouse models

Sun5$^{-/-}$ mice were generated in cooperation with Wuhan Kangweida Company via TALEN technology. The mice were kept under specific pathogen-free (SPF) conditions. All animal experiments were approved by the Ethics Committee of the Department of Laboratory Animals, Central South University (CSU-2022-01-0087) and were performed according to laboratory animal management practices. Genomic DNA was extracted from mouse tail tip biopsy specimens. Then, genotypes were detected by PCR using the following *Sun5*-specific primers: F: 5′-CCCAGTGTCCAGGGATGAC ATTAA-3′, R: 5′-TGGGTCCACAGAAGGAAGGCA-3′. Finally, the PCR products were sequenced, and the results were compared with the gene sequences of the wild-type (WT) mice on the NCBI website.

RNA extraction and real-time quantitative PCR (qPCR) analyses

Total RNA was extracted from mouse testis tissue using TRIzol Reagent (Invitrogen, Carlsbad, USA). The first cDNA strand was synthesized according to the protocol for ReverTra Ace qPCR RT Master Mix with gDNA Remover (TOYOBO, Shanghai, China). The qPCR was performed using specific primers with TB Green Premix

Ex TaqTMII (Takara, Kyoto, Japan) on a qPCR instrument (Roche LightCycler 480; Roche, Basel, Switzerland). *Gapdh* was used as an internal control. Each experiment was repeated at least three times.

In situ hybridization

Testicular samples obtained from 8-week-old wild-type (WT) and *Sun5*$^{-/-}$ mice were fixed with 4% paraformaldehyde, dehydrated, paraffin-embedded and sectioned. Cell climbing sheets were prepared. RNA-FISH experiments were performed according to the manufacturer's protocol provided by Stellaris FISH Probes (RiboBio, Guangzhou, China) as previously described [23]. Briefly, after fixation with 4% paraformaldehyde, permeabilization was performed in 1× PBS containing 0.5% Triton X-100 (Sigma, Steinheim, Germany) at 4°C for 5 min. Blocking was performed by incubation in prehybridization buffer for 30 min at 37°C. Hybridization was performed with FISH probes using the Ribo™ Fluorescence *In Situ* Hybridization Kit (RiboBio) in a humid chamber at 37°C protected from light for more than 10 h. After washing, staining with DAPI was performed for 10 min in the dark. Oligo (dT, 50 dT) FISH probes were designed and synthesized by RiboBio. All images were obtained with a confocal microscope (Zeiss). The spermatogenic cells in three approximately sized lumens of testicular sections were counted for statistical purposes. Cell climbing sheets were counted by observing the poly (A)$^+$ RNA distribution of 100 cells in three separate experiments under each condition.

Haematoxylin-eosin staining

Epididymis samples obtained from 8-week-old WT and *Sun5*$^{-/-}$ mice were fixed with 4% paraformaldehyde. Haematoxylin and eosin staining was performed after dehydration, paraffin embedding and sectioning. Finally, the sections were observed and photographed under a microscope (Zeiss). In sperm smears, six separate experiments were performed, each in which 100 spermatozoa were counted for statistical purposes to analyze the morphological abnormalities of spermatozoa.

Motility assessment

Human tubal fluid (HTF; Aibei Biotechnology, Nanjing, China) was added to a sterile EP tube and equilibrated overnight in an incubator at 37°C and 5% CO_2. Cervical dislocation was used to kill adult male mice, after which the epididymal tissue was dissected and carefully removed. The tail of the epididymis was cut vertically, put into HTF solution, which was balanced in advance, and incubated at 37°C for 20 min. Then, 4 μL of HTF supernatant containing sperm was removed, and the tube was filled with a 20-μm sperm counting plate (for mice). Sperm motility was assessed through a computer-assisted sperm analyzer (CASA; Saisi, Beijing, China). Three technical replicates were examined with 500 sperm per replicate.

Cell culture

The mouse spermatocyte cell line GC-2 and human colon cancer cells (LoVo cells) were purchased from the ATCC. All cells were cultured in Dulbecco's modified Eagle's medium (DMEM; Gibco, Carlsbad, USA) supplemented with 10% FBS and maintained in a 5% CO_2 cell culture incubator at 37°C.

Interference of *Sun5*

The lentivirus containing *Sun5* was obtained from Tsingke Biotech (Beijing, China). To construct stable *Sun5*-knockdown cell lines, GC-2 cells or LoVo cells were transfected with lentivirus expressing the *Sun5*-shRNA sequence (GATGACAGCATAAATGGTCCA; Tsingke Biotech). After 72 h, the cells were observed under a fluorescence microscope to assess the infection efficiency. Then, the cells were selected with 2 μg/mL puromycin. Finally, the efficiency in different cells was determined by western blot analysis.

Nuclear and cytoplasmic fractionation

The cells were collected and then precipitated by centrifugation (800×*g* for 10 min). The cells were washed with PBS 3 times and centrifuged at 500 *g* for 5 min at 4°C. The corresponding volume of lysis buffer was added according to the volume of the compacted cells. The remaining steps were performed according to the protocol of the nuclear and cytoplasmic protein extraction kit (Solarbio, Beijing, China). The experiment was independently repeated 3 times.

Statistical analysis

Statistical analyses were performed using GraphPad PRISM version 8 (GraphPad Software, La Jolla, USA), and the statistical significance of differences between groups was calculated by Student's *t* test. The online website (https://www.xiantaozi.com/literatures) was used to perform KEGG and GO enrichment analyses of the IP-MS results.

Results

Sun5 interacts with hnRNP F/H1 and hnRNP K and is involved in mRNA export

To clarify the molecular mechanism of SUN5 in spermatogenesis, we carried out IP-MS to screen for proteins potentially interacting with *Sun5* in WT(C57BL/6J)mouse testes at 8 weeks postnatal. A total of 206 proteins were obtained for subsequent analyses. Kyoto Encyclopedia of Genes and Genomes (KEGG) online analysis suggested that the identified proteins may be involved in the process of RNA transport (Figure 1A). Furthermore, the Gene Ontology (GO) enrichment results indicated that these proteins may participate in RNA biological processes such as RNA transport, mRNA binding, and poly(A) binding (Figure 1B).

Based on the IP-MS results, the identified proteins included hnRNPs (hnRNP F/H1 and hnRNP K), Nxf1 and Nup93, most of which have been confirmed to participate in mRNA export (Figure 1C). Then, we performed co-IP to confirm the interaction between SUN5 and hnRNPs by using an anti-Flag antibody. In the immunoprecipitates of SUN5-Flag NTERA-2 cells, both SUN5 and hnRNPs, including hnRNP F/H1 and hnRNP K, were detected by western blot analysis (Figure 1D). Moreover, the interaction between *Sun5* and hnRNPs in WT mouse testis lysates was verified by co-IP (Figure 1D). Furthermore, we showed the localization of these proteins by immunofluorescence staining. HnRNP F/H1 and hnRNP K were present mainly in the nucleus. The fluorescence results showed that *SUN5*, which was labeled with green fluorescence, and hnRNPs (hnRNP F/H1 and hnRNP K), which were labeled with red fluorescence, colocalized to the nuclear membrane (Figure 1E). Thus, combined with the results of the bioinformatics IP-MS analyses, we speculated that *Sun5* may participate in mRNA export.

RNA fluorescence *in situ* hybridization (FISH) reveals the accumulation of poly(A)$^+$ RNA in the nucleus during spermatogenesis in *Sun5*$^{-/-}$ mice

Acephalic spermatozoa syndrome (ASS) is a rare reproductive and genetic disease that is resulted from the mutation of genes, such as

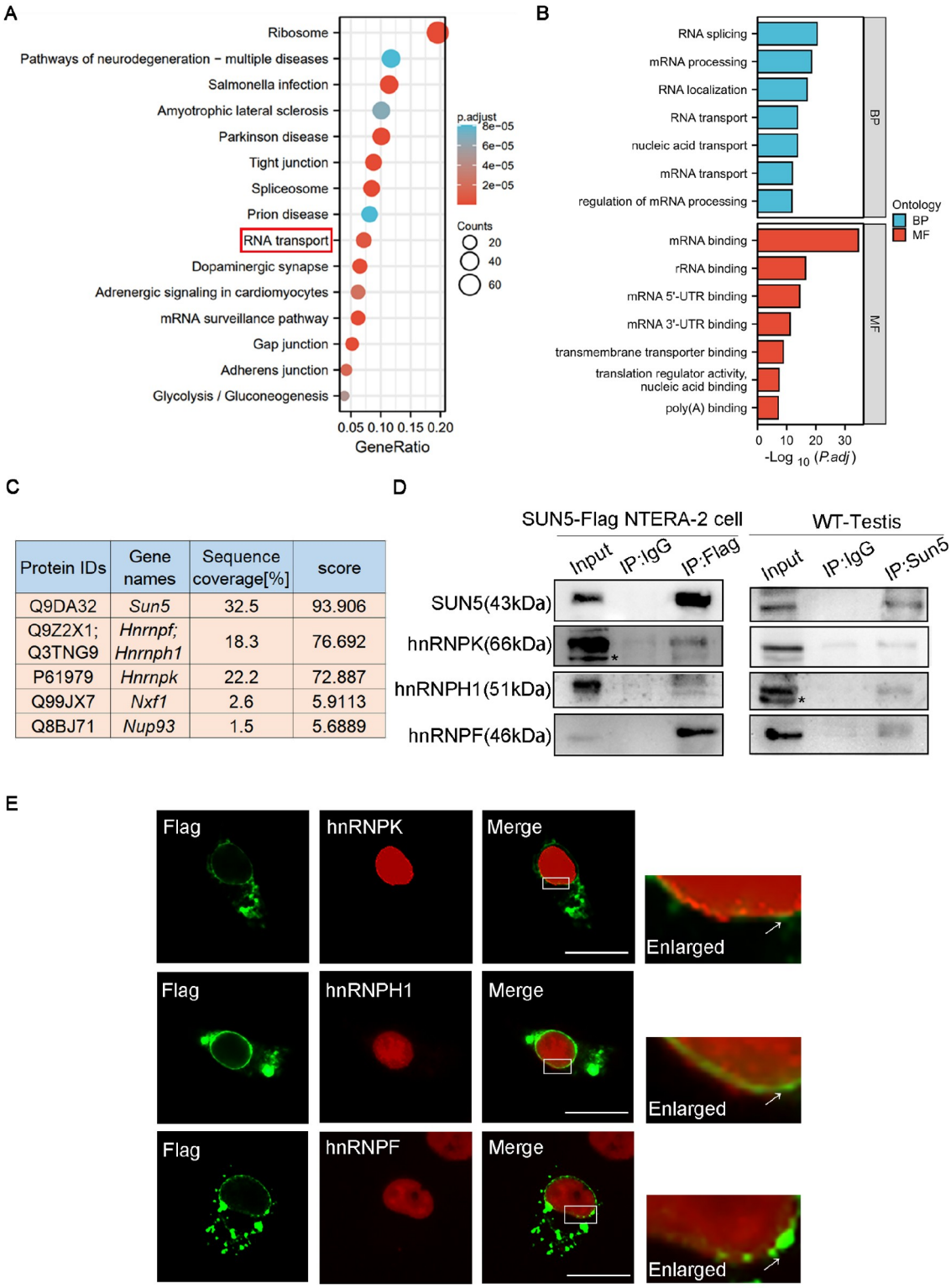

Protein IDs	Gene names	Sequence coverage[%]	score
Q9DA32	*Sun5*	32.5	93.906
Q9Z2X1; Q3TNG9	*Hnrnpf; Hnrnph1*	18.3	76.692
P61979	*Hnrnpk*	22.2	72.887
Q99JX7	*Nxf1*	2.6	5.9113
Q8BJ71	*Nup93*	1.5	5.6889

Figure 1. SUN5 interacts with hnRNP F/H1 and hnRNP K and is involved in mRNA export (A) Kyoto Encyclopedia of Genes and Genomes (KEGG) online analysis of proteins screened by IP-MS. (B) Gene Ontology (GO) enrichment of proteins screened by IP-MS. (C) Data of some proteins interacting with SUN5 identified by IP-MS. (D) Interaction between SUN5 and hnRNPs (hnRNP K, hnRNP H1, hnRNP F). The black asterisks (*) indicate nonspecific bands. (E) Colocalization of SUN5 with hnRNP F/H1 or hnRNP K. SUN5-Flag NTERA-2 cells were stained with suitable antibodies and analyzed via confocal microscopy. Scale bar: 15 μm.

PMFBP1 [24] and *Sun5* [25]. Approximately 33% ~ 47% of patients with ASS have *SUN5* gene mutations, but the underlying molecular mechanism is not clear. To further elucidate the function of *SUN5*, we generated *Sun5*-knockout ($Sun5^{-/-}$) mice by applying TALEN technology to edit exon 4 (Figure 2A). Compared with those in WT mice, 8 bases in exon 4 were replaced by a single base, T, in $Sun5^{-/-}$ mice. The genotype of homozygous *Sun5*-knockout mice was verified by sequencing (Figure 2B). However, a 7-base deletion may result in frameshift or abnormal alternative splicing. *Sun5* expression was downregulated at both the protein and mRNA levels in $Sun5^{-/-}$ mice, as shown by western blot analysis and qPCR, suggesting that the mouse model was constructed successfully ($P<0.05$, Figure 2C–D).

To investigate whether knockout of *Sun5* causes abnormal mRNA export in spermatogenesis, we examined the cellular distribution of poly (A)$^+$ RNA in testicular sections of WT and $Sun5^{-/-}$ mice of the same week of age by RNA fluorescence *in situ* hybridization with an oligo probe. Fluorescence staining revealed that poly (A)$^+$ RNA was mainly distributed in the cytoplasm, and a small amount was distributed in the nucleus in spermatocytes and secondary spermatocytes of the WT (Figure 2E–G). In contrast, most poly(A)$^+$ RNA accumulated in the nucleus, and few were distributed in the cytoplasm in spermatocytes and secondary spermatocytes of $Sun5^{-/-}$ mice ($P<0.0001$, $n=3$, Figure 2E–G). In particular, in round spermatids, poly (A)$^+$ RNA aggregated in the cytoplasm for transient storage in the WT; however, it diffused into the nucleus in $Sun5^{-/-}$ mice ($P<0.0001$, $n=3$; Figure 2E,H). Generally, the distribution of poly (A)$^+$ RNA is altered in $Sun5^{-/-}$ mice, which indicates that *Sun5* depletion results in decreased mRNA export during spermatogenesis.

Sun5 knockout in mice leads to abnormal spermatogenesis by affecting spermatogenesis-related protein expression

The export of mRNA from the nucleus to the cytoplasm affects protein expression. To observe the effect of *Sun5* deficiency on the profile of testicular protein expression, iTRAQ was performed to demonstrate that the expression of some spermatogenesis-related proteins was altered in *Sun5*-knockout mice. To verify this result, we selected Odf1, Odf2, and Akap4 (A-kinase anchor protein 4) for validation and found that these genes were downregulated at both the protein and mRNA levels in $Sun5^{-/-}$ mice by western blot analysis and qPCR (Figure 3A,B). According to the above data, *Sun5* is involved in mRNA export and specifically regulates the expression of spermatogenesis-related genes.

Subsequently, we histologically stained the epididymides of the WT and $Sun5^{-/-}$ mice. The haematoxylin-eosin staining results demonstrated that the epididymal lumen of the WT was filled with blue-stained spermatozoa heads, while this effect was rarely observed in $Sun5^{-/-}$ mice (Figure 3C). Furthermore, detailed examination of the morphology of mature spermatozoa in the seminiferous tubules revealed that approximately 98% of the sperm components were headless flagella, and the remaining were sperm heads only or sperm with abnormal head–tail junctions ($P<0.0001$, Figure 3D). Moreover, we found that motile spermatozoa and progressive motile spermatozoa were both significantly decreased in $Sun5^{-/-}$ mice by using the CASA system ($P<0.0001$, Figure 3E and Supplementary Videos S1,S2). Taken together, these results indicated that *Sun5* knockout downregulated the expressions of spermatogenesis-related genes, resulting in reduced sperm counts, decreased sperm motility and disrupted sperm head-to-tail junctions, which is similar to the phenotype of ASS in humans.

Poly (A)$^+$ RNA, hnRNP F/H1, and hnRNP K accumulate in the nucleus of *Sun5* knockdown cells

To further confirm that *Sun5* can regulate mRNA export, we established stable *Sun5*-knockdown cells (GC-2 cells transfected with the PLV3ltr-ZsGreen-Puro-U6-shSUN5 lentivirus). Western blot analysis results showed that *Sun5* was significantly downregulated in the *Sun5*-knockdown (also called shSun5) group ($P<0.05$, Figure 4A). The immunofluorescence staining results showed that poly(A)$^+$ RNA was mainly distributed in the cytoplasm of cells in the control group. Compared with the control, poly(A)$^+$ RNA was significantly retained in the nucleus of *Sun5*-knockdown cells, which was similar to what we observed in the testes of $Sun5^{-/-}$ mice (Figure 4B). Shuttle hnRNPs, such as hnRNP K, accompany mRNA into the cytoplasm through the NPC, so they have become important markers of mRNA export efficiency [26]. To test whether *Sun5* knockdown influences the distribution of hnRNPs, we extracted the cytoplasm and nuclei of control and *Sun5*-knockdown cells. Lamin B1 and GAPDH were used as nuclear and cytosolic markers, respectively. Interestingly, based on the levels of Lamin B1 and GAPDH, both hnRNP F/H1 and hnRNP K appeared to be decreased in the cytosolic fraction of *Sun5*-knockdown cells and increased in the nuclear fraction compared to those in control cells ($P<0.05$, Figure 4C,D). In addition, we constructed *SUN5*-knockdown LoVo cells and observed a similar phenomenon in which poly (A)$^+$ RNA, hnRNP F/H1 and hnRNP K simultaneously accumulated in the nucleus ($P<0.05$, Supplementary Figure S1). In general, knockdown of *Sun5* caused poly (A)$^+$ RNA and hnRNPs (hnRNP F/H1 and hnRNP K) to be retained in the nucleus, resulting in an obstruction of mRNA export from the nucleus.

Sun5 participates in mRNA export by interacting with Nxf1 and Nup93

As a general mRNA export factor, NXF1 binds to mature mRNP substrates in the nucleoplasm and then transports the mRNP to the cytoplasm. Based on the IP-MS results, SUN5 may interact with Nxf1 in the mouse testis. We performed co-IP by using an anti-Flag antibody or anti-NXF1 antibody and detected SUN5 and NXF1 in the sediment of SUN5-Flag NTERA-2 cells (Figure 5A). Similarly, both SUN5 and Nxf1 were detected in immunoprecipitates of mouse testes by using an anti-SUN5 antibody (Figure 5B). These data suggest that the nuclear membrane protein SUN5 interacts with Nxf1 and recruits Nxf1-binding mRNPs to the nuclear membrane.

The Nxf1-binding mRNP complex, which directly targets the NPC or is recruited to the nuclear envelope and then presented to the NPC, is transported to the cytoplasm through the central channel of the NPC [4,17]. As components of the NPC, nucleoporins, such as Nup153 [17], Nup155 [19], and Nup188 [20], also participate in mRNA transport. IP-MS revealed that Nup93 is a potential protein that interacts with SUN5 in mice. Subsequently, Co-IP was performed to verify the interaction between SUN5 and Nup93 in cells and in mice. By using an anti-Flag antibody and anti-NUP93 antibody for precipitation, both SUN5 and NUP93 were detected in the immunoprecipitates of mouse testicular lysates (Figure 5B). Moreover, we verified the interaction between SUN5 and Nup93 in SUN5-Flag NTERA-2 cells by using an anti-SUN5 antibody

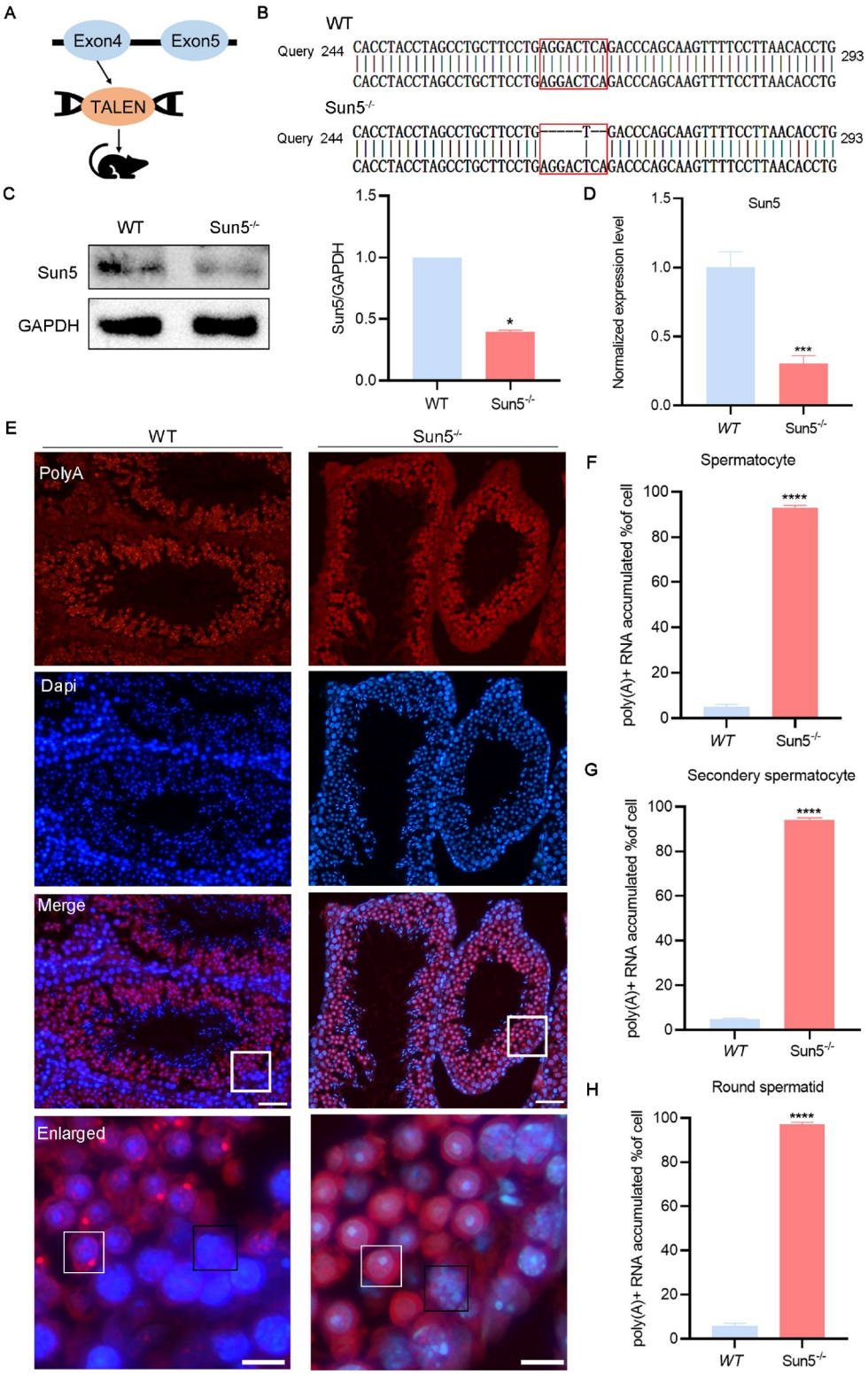

Figure 2. RNA fluorescence *in situ* hybridization reveals nuclear accumulation of poly (A)$^+$ RNA during spermatogenesis in *Sun5*$^{-/-}$ mice (A) Schematic illustration of the *Sun5*$^{-/-}$ mouse strategy. (B) Sequences of the mutation alleles in *Sun5*$^{-/-}$ mice determined by Sanger sequencing. (C,D) Western blot analysis and qPCR results showing the downregulation of *Sun5* in the testes of *Sun5*$^{-/-}$ mice. GAPDH was used as a loading control. (E) RNA fluorescence *in situ* hybridization of testis sections from adult WT and *Sun5*$^{-/-}$ mice. Scale bars: upper panel, 50 μm; lower panel, 15 μm. The white rectangles represent round spermatids, and the black rectangles represent spermatocytes in WT and *Sun5*$^{-/-}$ mice. (F–H) The percentage of poly(A)$^+$ RNA that accumulated in the nuclei of spermatocytes (F), secondary spermatocytes (G), and round spermatids (H) in WT and *Sun5*$^{-/-}$ mice. Data are presented as the mean±SEM, n=3. *P<0.05, **P<0.01, ***P<0.001, ****P<0.0001.

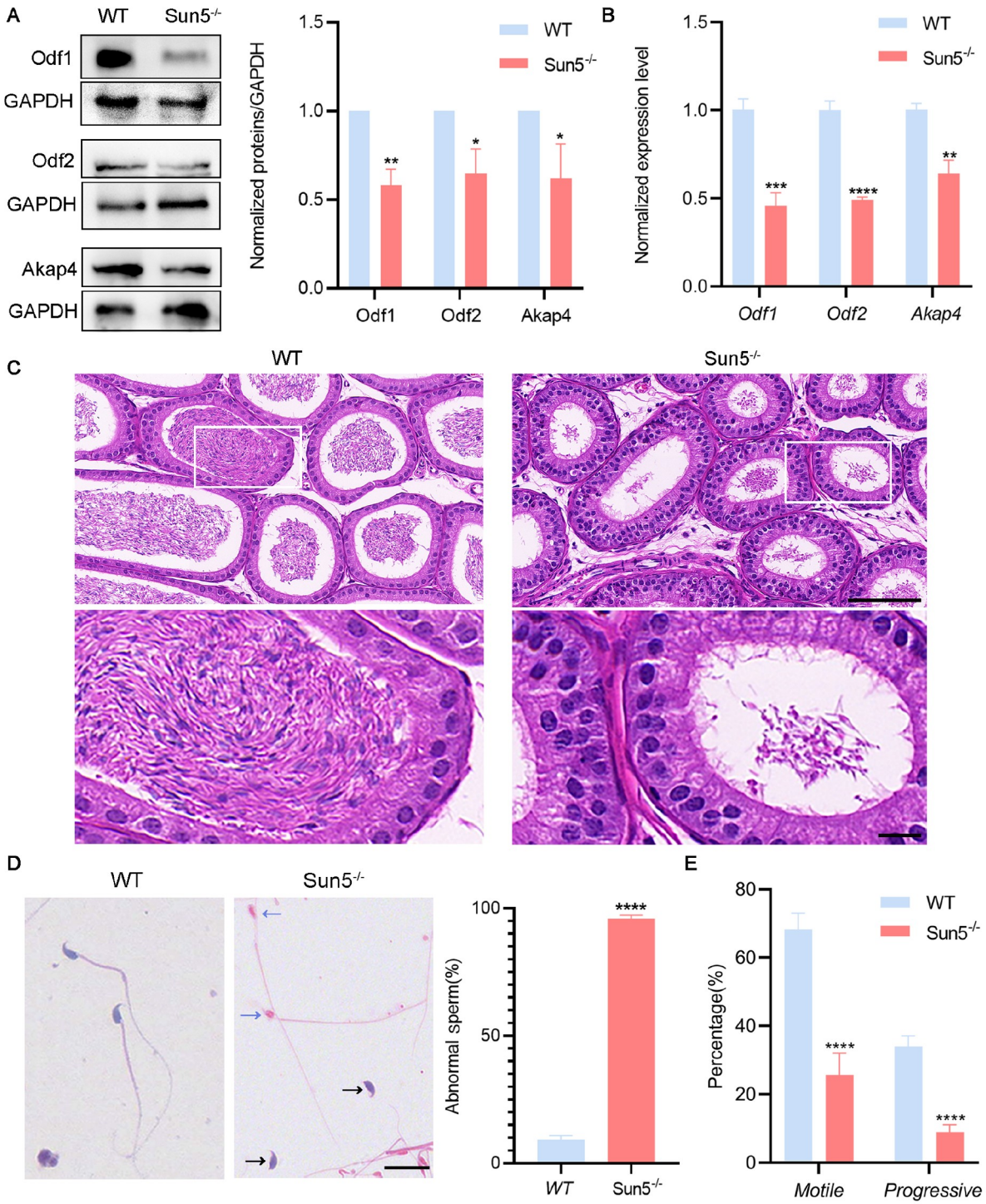

Figure 3. Knockout of *Sun5* in mice leads to abnormal spermatogenesis by affecting spermatogenesis-related protein expression (A) Validation of genes related to spermatogenesis at the protein level in *Sun5*$^{-/-}$ mice. (B) Validation of genes related to spermatogenesis at the mRNA level. (C) Hematoxylin-eosin (HE) staining of the WT and *Sun5*$^{-/-}$ mice. Scale bars: upper panel, 100 μm; lower panel, 20 μm. (D) The results of HE staining of mouse epididymis sperm smears. The black arrows represent scattered sperm heads, and the blue arrows represent headless sperm. Scale bar: 20 μm. The percentage of abnormal sperm in WT and *Sun5*$^{-/-}$ mice (n=6). (E) The CASA results of WT and *Sun5*$^{-/-}$ mice indicated that the numbers of motile spermatozoa and progressive motile spermatozoa both decreased in *Sun5*$^{-/-}$ mice (n=3). Data are presented as the mean±SEM. *P<0.05, **P<0.01, ***P<0.001, ****P<0.0001.

(Figure 5C). The above results indicated that SUN5 presents Nxf1-binding mRNPs to the NPC by interacting with Nup93.

To determine whether Nup93 is involved in mRNA export, we constructed an *Nup93*-knockdown GC-2 cell line via siRNA. Western blot analysis confirmed the efficient knockdown of *Nup93* in GC-2 cells (P<0.01, Figure 5D). Compared with those in

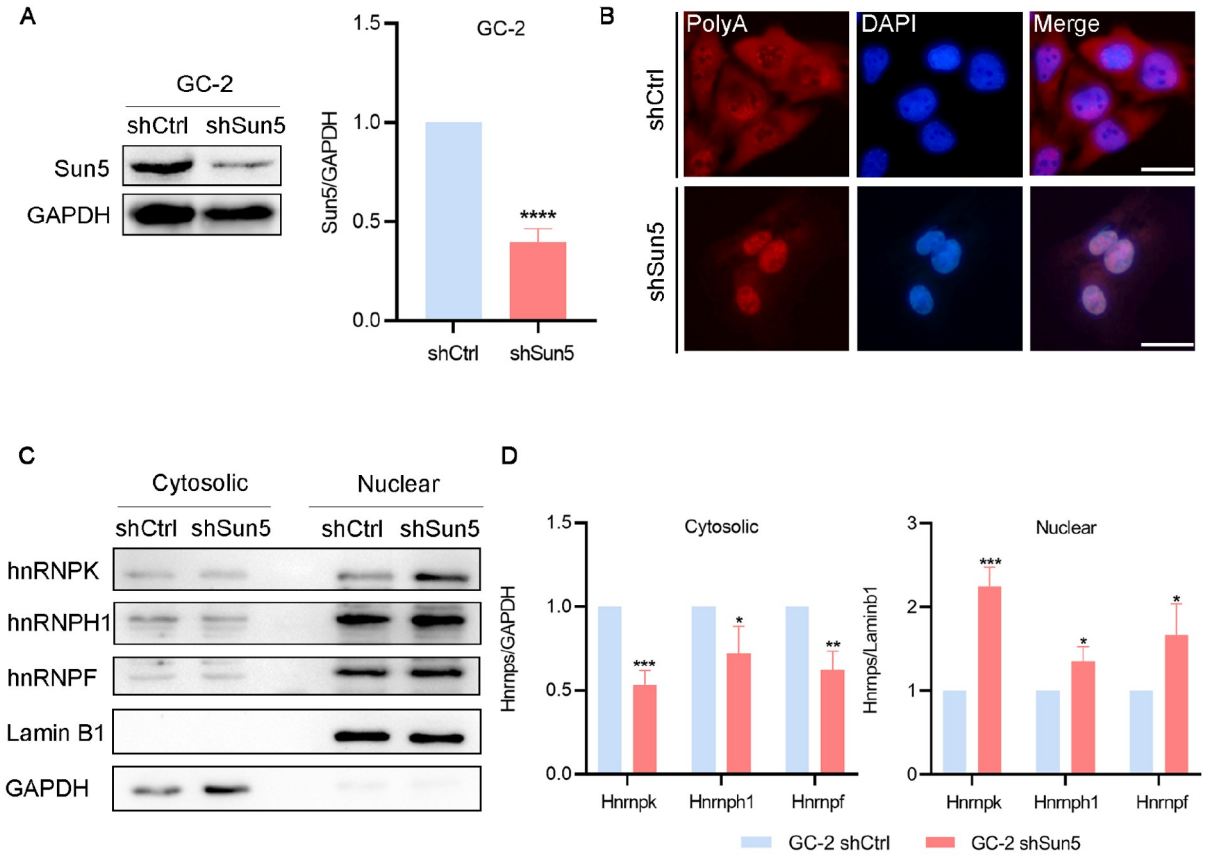

Figure 4. Poly(A)$^+$ RNA, hnRNP F/H1, and hnRNP K accumulate in the nucleus in *Sun5*-knockdown cells (A) Western blot analysis of SUN5 expression levels in control and *Sun5*-knockdown cells. GAPDH was used as a loading control. (B) *Sun5* deficiency results in the nuclear accumulation of poly (A)$^+$ RNA. RNA FISH showed poly (A)$^+$ RNA accumulation in the nucleus of *Sun5*-depleted cells after lentivirus transfection. Scale bar: 15 μm. (C) Separation of nuclear and cytoplasmic proteins by subcellular fractionation in control and *Sun5*-knockdown cells. Lamin B1 and GAPDH were used as nuclear and cytosolic markers, respectively. (D) Statistical analysis of subcellular fractionation in (C). Data are presented as the mean±SEM, n=3. *P<0.05, **P<0.01, ***P<0.001.

control cells, poly(A)$^+$ RNA in *Nup93*-knockdown cells significantly aggregated in the nucleus according to *in situ* fluorescence hybridization (Figure 5E). Furthermore, we extracted the cytoplasm and nuclei of control and *Nup93*-knockdown cells. Compared to those in control cells, both hnRNP F/H1 and hnRNP K decreased in the cytosolic fraction and increased in the nuclear fraction of *Nup93*-knockdown cells based on the levels of Lamin B1 and GAPDH (P<0.05, Figure 5F,G). Lamin B1 and GAPDH were used as nuclear and cytosolic markers, respectively. According to the above experimental results, Nup93 is involved in the export of mRNA. Taken together, these data indicated that there is a novel mRNA export chain of Nxf1/SUN5/Nup93 in germ cells, and we proposed the following model: SUN5 recruits Nxf1-binding mRNP to the nuclear membrane and hands it to Nup93, allowing the export of nuclear mRNAs to proceed smoothly.

Sun5 functions in NXF1-dependent mRNA export

There are two pathways for mammalian RNA export, the NXF1-dependent pathway and the CRM1-dependent pathway. To determine which export pathway SUN5 is involved in, we used leptomycin B (LMB) to block CRM1-dependent export.

By comparing the distribution of poly(A)$^+$ RNA in LMB-untreated cells, we observed that poly(A)$^+$ RNA was mainly distributed in the cytoplasm in the control group; however, it significantly aggregated in the nucleus after *Sun5* knockdown, suggesting that SUN5 is involved in mRNA export (P<0.001, n=3, Figure 6A,B). Furthermore, by comparing the distribution of poly(A)$^+$ RNA in both LMB-untreated and LMB-treated controls, we demonstrated that poly(A)$^+$ RNA was significantly clustered in the nucleus in the LMB-treated control group (P<0.01, n=3, Figure 6A,C), indicating that LMB treatment effectively inhibited the expression of this mRNA through CRM1-dependent nuclear export. Comparison of the distribution of poly(A)$^+$ RNA in both LMB-untreated and LMB-treated *Sun5*-knockdown cells revealed that the aggregation of poly(A)$^+$ RNA in the nucleus was intensified after LMB treatment, suggesting that LMB treatment could still inhibit the CRM1 pathway in the *Sun5*-knockdown group, which indirectly indicated that Sun5 could regulate mRNA export through the NXF1 pathway (P<0.01, n=3; Figure 6A,D). We performed similar experiments in LoVo cells and obtained the same results (Supplementary Figure S2). Based on these data, we concluded that SUN5-mediated regulation of the nuclear export of mRNA mainly depends on an NXF1-dependent pathway.

Knockout of *Sun5* inhibits the process of Nxf1 binding to Nup93 by mRNPs

To investigate the effect of *Sun5* on mRNA export in detail, we

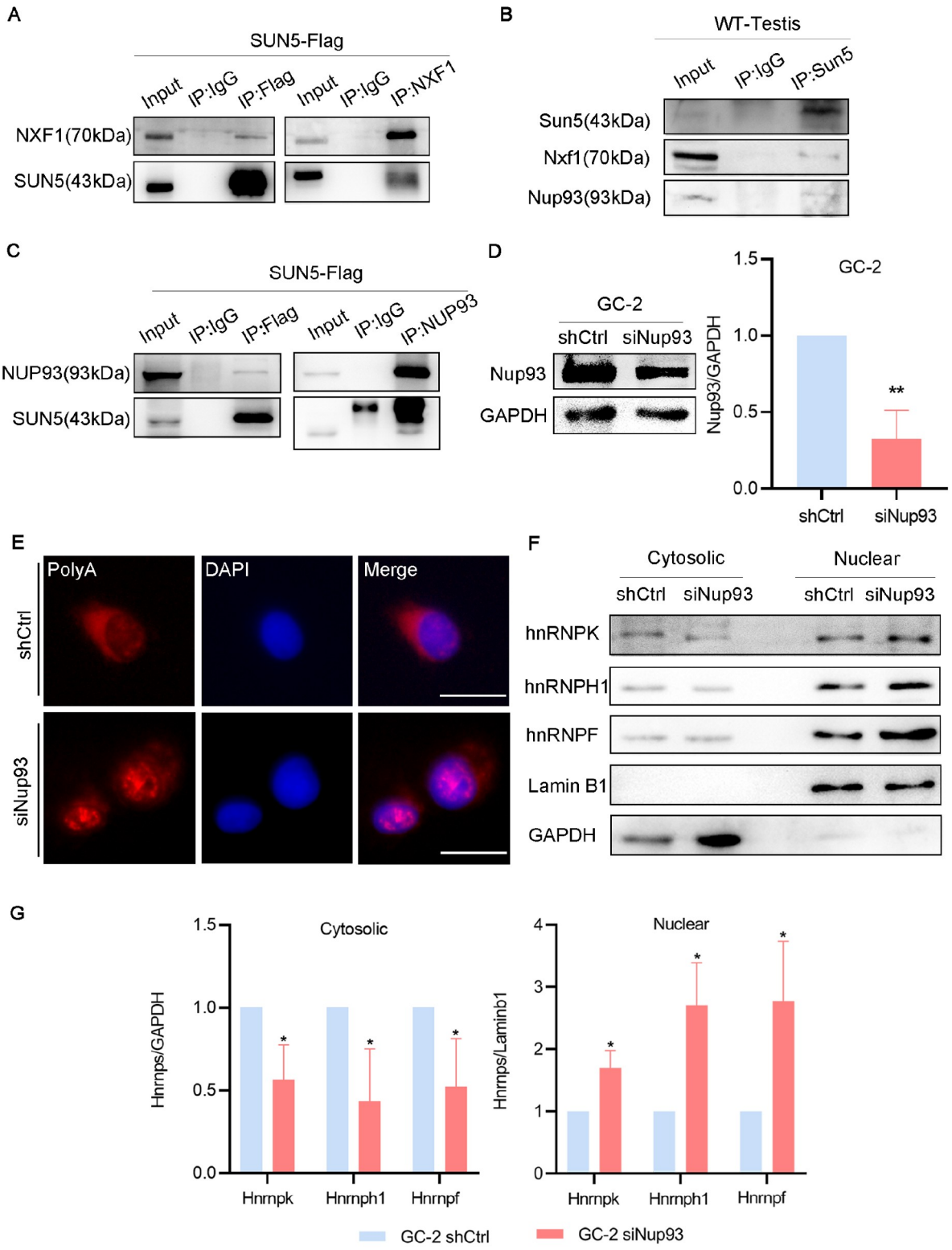

Figure 5. SUN5 participates in mRNA export by interacting with Nxf1 and Nup93 (A,B) Interaction between SUN5 and NXF1 or NUP93 in SUN5-Flag NTERA-2 Cell identified by Co-IP. (C) The interaction between SUN5 and Nxf1 or Nup93 in mouse testes identified by Co-IP. (D) Western blot analysis of Nup93 expression levels in control and Nup93 siRNA cells. GAPDH was used as a loading control. (E) Nup93 interference results in the nuclear accumulation of poly $(A)^+$ RNA. Scale bar: 15 μm. (F) Separation of cytoplasmic and nuclear proteins in control and Nup93 siRNA cells by subcellular fractionation. GAPDH and Lamin B1 were used as cytosolic and nuclear markers, respectively. (G) Statistical analysis of subcellular fractionation in (F). Data are presented as the mean±SEM, n=3. *P<0.05, **P<0.01.

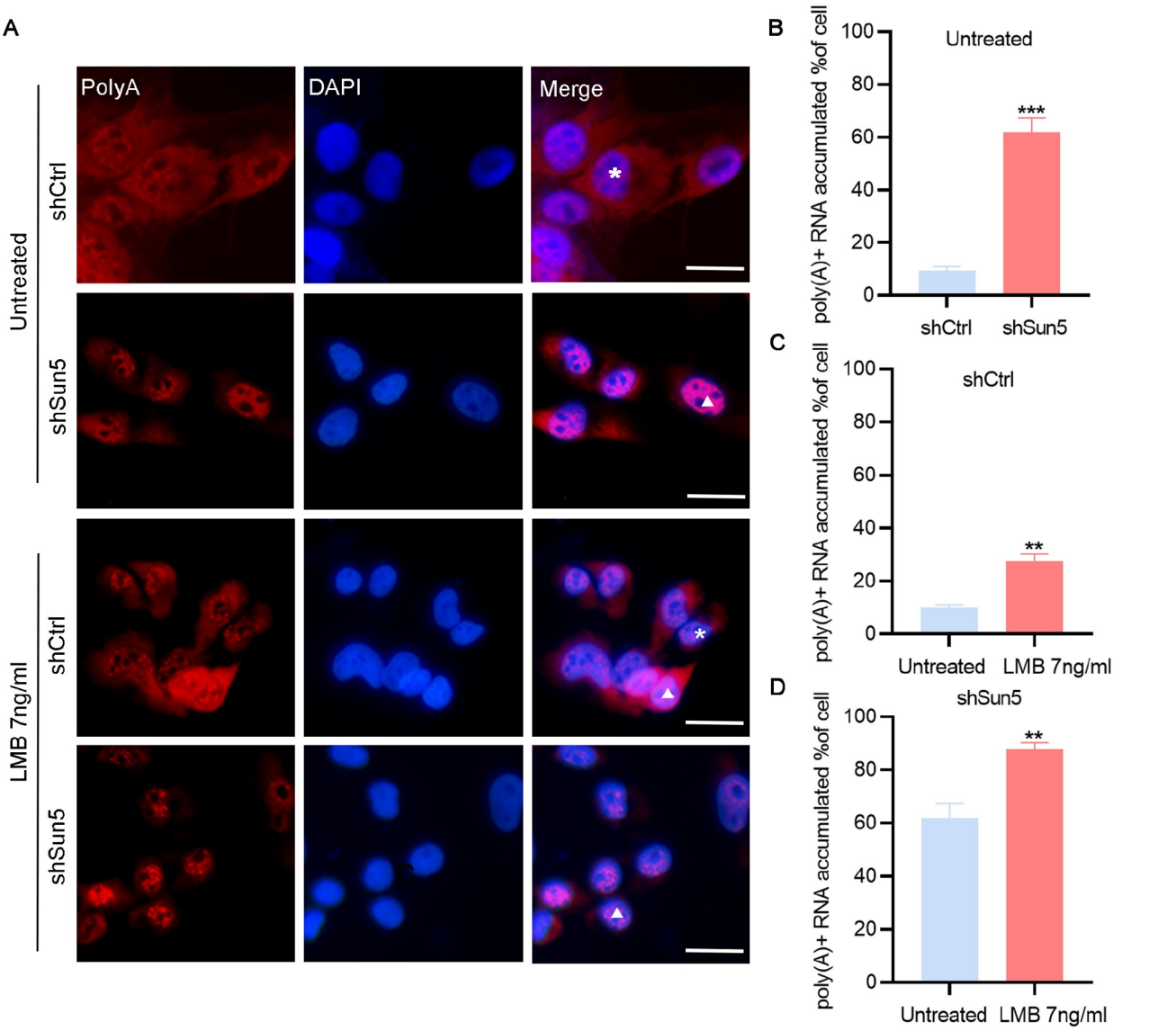

Figure 6. SUN5 functions in NXF1-dependent mRNA export (A) RNA FISH showing the distribution of poly (A)$^+$ RNA in both LMB-untreated and LMB-treated cells, including control and *Sun5*-knockdown cells. Treatment was performed by incubation with 7 ng/mL LMB for 2 h. Scale bar: 15 μm. (B) The percentage of poly (A)$^+$ RNA that accumulated in the nucleus of untreated control and *Sun5*-knockdown cells. (C) The percentage of poly (A)$^+$ RNA that accumulated in the nucleus of LMB-untreated and treated control cells. (D) The percentage of poly (A)$^+$ RNA that accumulated in the nucleus of untreated and treated *Sun5*-knockdown LMB cells. One hundred cells were counted independently, n=3. Data are presented as the mean±SEM. $^{**}P$<0.01, $^{***}P$<0.001.

carried out western blot analysis to observe the protein expressions of Nxf1 and Nup93 in *Sun5*$^{-/-}$ mice. Compared with those in the testes of WT mice, the expressions of Nxf1 and Nup93 in the testes of *Sun5*$^{-/-}$ mice did not change (P>0.05, Figure 7A). Similarly, compared to those in the control group, the expressions of Nxf1 and Nup93 in *Sun5*-knockdown GC-2 cells did not change (P>0.05, Figure 7B). These data indicated that knockdown of *Sun5* did not affect the expression of Nxf1 or Nup93 but rather impeded mRNA export by affecting other steps.

As a nuclear membrane protein, *Sun5* recruits Nxf1-binding mRNPs to the nuclear membrane and transfers them to Nup93. Subsequently, we examined the binding strength between Nxf1 and Nup93 in WT and *Sun5*$^{-/-}$ mouse testes and observed that Nxf1 binding was obviously attenuated in *Sun5*$^{-/-}$ mice (P<0.05, Figure 7C,E). Similarly, the binding of Nxf1 to Nup93 was reduced in *Sun5*-knockdown GC-2 cells compared with control cells (P<0.05, Figure 7D,E). Therefore, due to the downregulation of SUN5 expression, the process of submitting Nxf1-binding mRNPs to Nup93 is inhibited, resulting in an obstruction of mRNA export. Overall, SUN5-mediated nuclear mRNA export may be a novel pathway of mRNA export in male germ cells.

Discussion

The export of mRNA from the nucleus to the cytoplasm is a complicated process. During spermatogenesis, many testis-specific genes play roles in physiological mRNA processes, including mRNA export. In the present study, we generated *Sun5*$^{-/-}$ mice and observed that poly(A)$^+$ RNA accumulated in the nuclei of germ

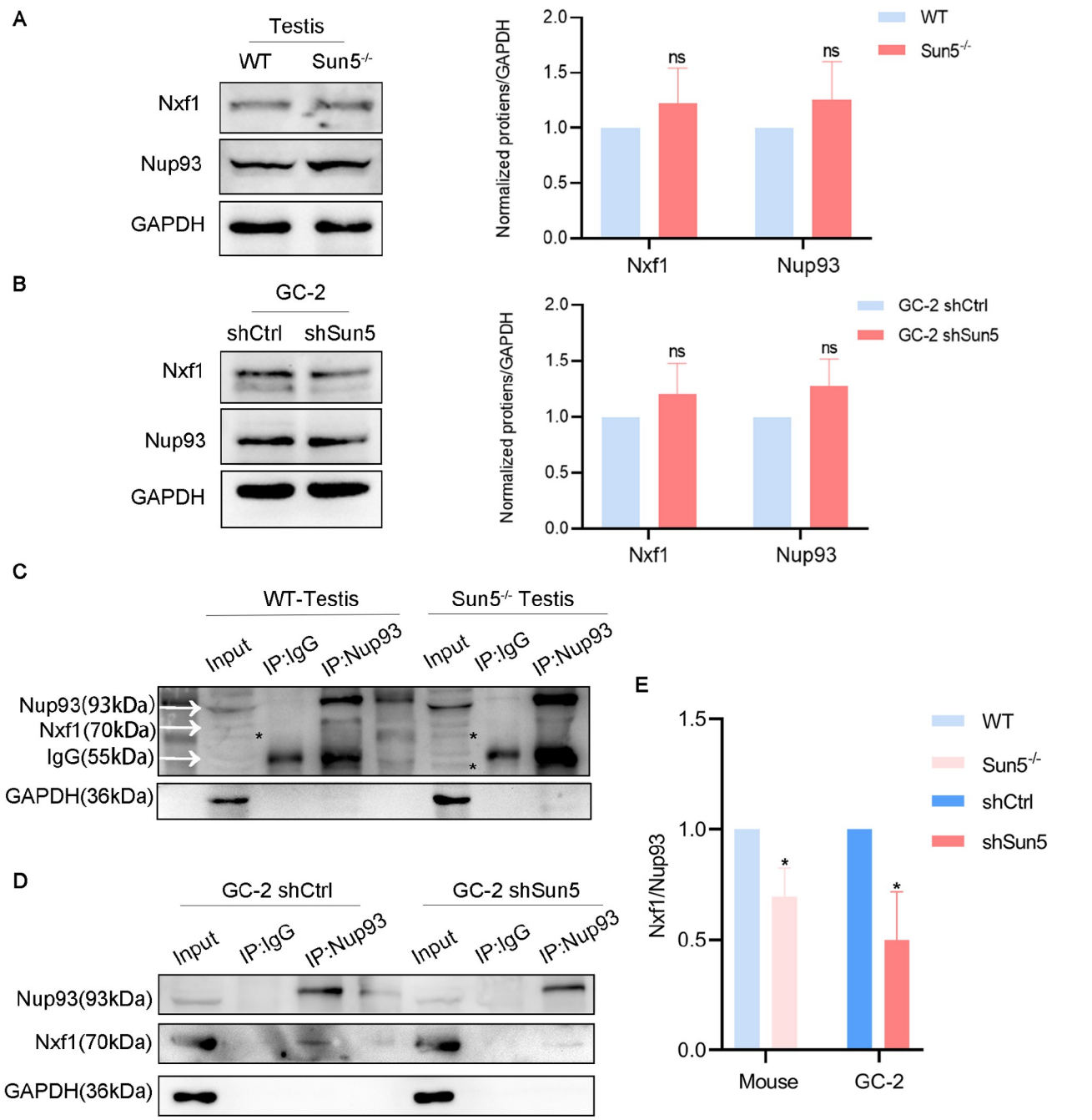

Figure 7. Knockout of *Sun5* inhibits the process of Nxf1 binding to Nup93 (A) Western blot analysis results showing the protein levels of Nxf1 and Nup93 in the testis tissues of WT and *Sun5*$^{-/-}$ mice. (B) Western blot analysis results showing the protein levels of Nxf1 and Nup93 in control and *Sun5*-knockdown GC-2 cells. (C,D) The binding strength of Nxf1 and Nup93 in WT and *Sun5*$^{-/-}$ mouse testes (C) and in control and *Sun5*-knockdown GC-2 cells (D). The black asterisks (*) indicate nonspecific bands. (E) Statistical analysis of (C) and (D). Data are presented as the mean± SEM, n=3. *P<0.05, *ns*: P>0.05.

cells, which caused the dysregulation of spermatogenesis-related genes, leading to reduced sperm counts, decreased sperm motility and disrupted sperm head-to-tail junctions. Mechanistically, SUN5 interacts with Nxf1 and Nup93 to form a novel mRNA export pathway, and the following model is proposed (as modeled in Figure 8): SUN5 recruits Nxf1-binding mRNP to the nuclear membrane and hands it over to Nup93, ensuring the smooth export of mRNA to the cytoplasm. These data provide new insights into mRNA export in male germ cells.

SUN5, acting as a docking point, recruits Nxf1-bound mRNP to the NE and hands it over to Nup93. When the expression of SUN5 is downregulated, the export of mRNA is impaired, which results in downregulated expressions of spermatogenesis-related proteins, such as Odf1, Odf2 and Akap4.

In the nucleus, DNA is transcribed to pre-mRNA, which combines with RBPs to form mRNPs [9]. mRNPs are subsequently exported to

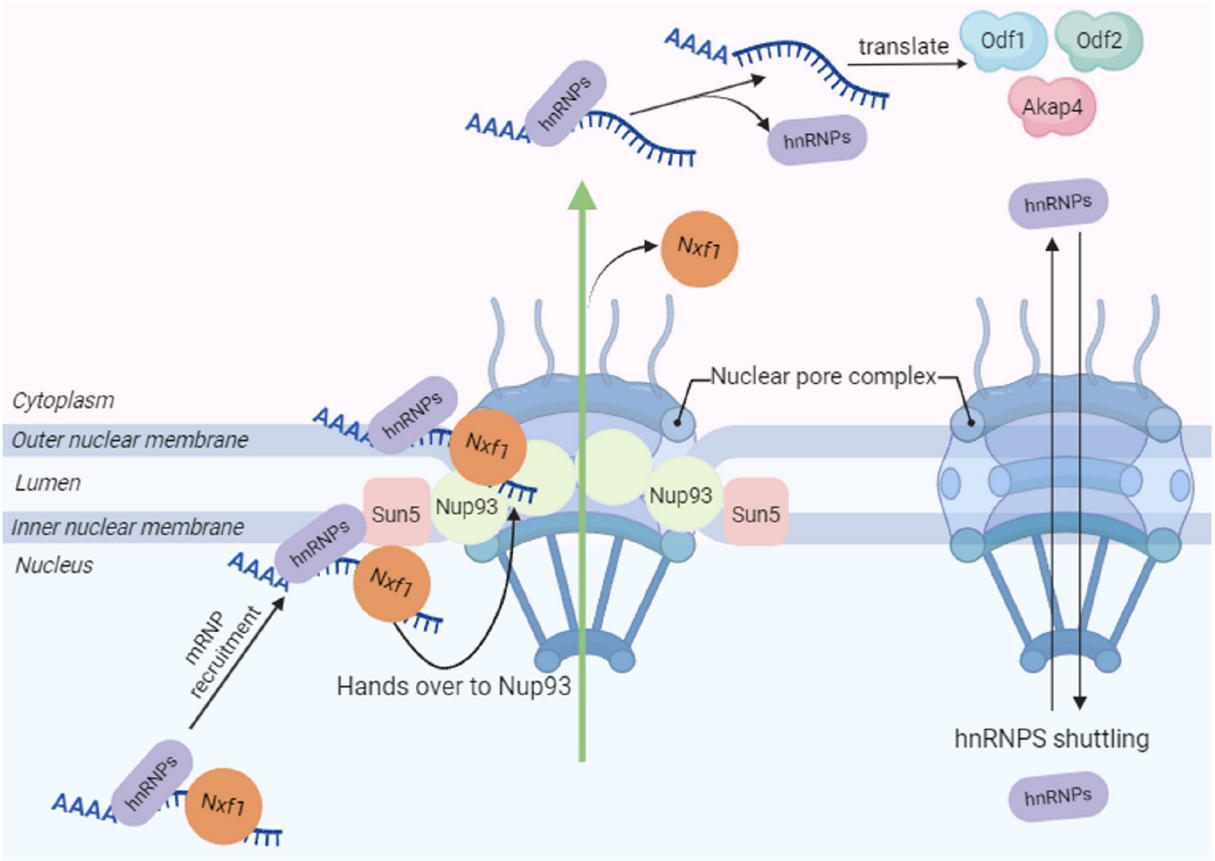

Figure 8. A model of SUN5 functions in mRNA export during spermatogenesis

the cytoplasm via two pathways: the CRM1 pathway and the NXF1 pathway [8]. In this study, we used LMB to block the CRM1-dependent pathway in GC-2 cells and observed that *Sun5*-knockdown cells showed additive accumulation of nuclear poly(A)$^+$ RNA after LMB treatment, indicating that the functions of SUN5 in mRNA export are dependent on the NXF1-dependent pathway.

The classical model of mRNA export suggests that NXF1 binds to mature mRNP substrates in the nucleoplasm and then employs mRNP to the cytoplasm via the NPC channel by interacting with FG repeats containing nucleoporins within the central NPC channel [4]. However, recent studies have also shown that NXF1 can interact with nucleoporins without FG repeat sequences, such as NUP358 [16,27]. As a nucleoporin, Nup93, which has no FG repeats, is localized in the central channel of the NPC [16]. Moreover, nucleoporins without FG repeat sequences, such as NUP155 [19] and NUP188 [20], are involved in mRNA export. Interference with Nup93 blocks mRNA export, suggesting that Nup93 is involved in mRNA export. In this study, we verified that Nxf1 interacts with Nup93 by co-IP in cells and in mouse testes. Therefore, upon the knockout/knockdown of *Sun5*, the submission of Nxf1-binding mRNPs to Nup93 via SUN5 is hindered, affecting mRNA export from the nucleus to the cytoplasm. In detail, although Nup93 has no FG repeats, it is also involved in mRNA export for the following two possible reasons: Nup93 may be directly involved in mRNA export by itself, which provides a new perspective that mRNA export may not depend on FG repeats; alternatively, Nup93 participates in mRNA export by influencing its interacting proteins, such as Nup62, which contains FG repeats and has been demonstrated to be involved in this process. This chain, which consists of Nxf1, SUN5 and Nup93, offers a novel way to export mRNA during spermatogenesis.

Previous studies have shown that nuclear membrane proteins are involved in mRNA export [28,29]. SUN5, which belongs to the SUN domain protein family, interacts with KASH domain proteins to form the LINC complex, which physically connects the nucleus to the cytoskeleton [30,31]. Among them, SUN1 and SUN2 are from the same origin, and SUN4 and SUN5 are from another ancestor [32]. SUN1 and SUN2 are downregulated in different tumors [33,34]; however, SUN4 and SUN5 are upregulated in a variety of cancers [35–38], which indicates that they perform different functions. A previous study revealed that SUN1 participates in nuclear mRNA export in HeLa cells [17]. SUN1 is nonspecific and is expressed in both somatic and germ cells, and knockout of *Sun1* causes severe defects in meiosis in mice, indicating that Sun1 regulates spermatogenesis in the early stages [39,40]. In contrast to SUN1, SUN5 is specifically expressed in the testis and is detected at all stages from spermatocyte to mature sperm in both humans and mice [41]. The expression of SUN5 is strictly regulated by growth, with high expression beginning at 3 weeks and the highest expression occurring at 4–5 weeks after birth.[42] Knockout of *Sun5* in mice mainly affects spermiogenesis. Especially in round sperm cells, poly(A)$^+$ RNA is largely retained in the nucleus in *Sun5*$^{-/-}$ mice, while poly(A)$^+$ RNA is stored in the cytoplasm in WT mice. Knockout of *Sun5* causes the downregulation of spermato-

genesis-related genes (*Akap4*, *Odf1*, *Odf2*, etc.) at the mRNA and protein levels, resulting in abnormal sperm head-to-tail connections and reduced sperm counts and motility. Thus, we speculate that SUN1 and SUN5 may be involved in mRNA export through different mechanisms. In addition, we found that Sun1 interference did not affect the protein level of hnRNP K, which is a shuttle hnRNP. However, knockout of *Sun5* led to the downregulation of hnRNP K, while hnRNP F/H1 remained unaffected (Supplementary Figure S3). In pachytene and diplotene spermatocytes, hnRNP K is expressed mainly in the nucleus, indicating that hnRNP K is involved in transcriptional regulation. However, in postmeiotic transition spermatocytes, hnRNP K is relocated from the nucleus to the cytoplasm, suggesting that hnRNP K is involved in posttranscriptional regulation [43]. The above data indicate that, unlike SUN1, SUN5 may affect spermatogenesis by regulating the expression of hnRNP K, but the underlying molecular mechanism is not yet clear.

In addition, we screened 34 downregulated proteins in *Sun5*$^{-/-}$ mice by iTRAQ, some of which are related to spermiogenesis but not all, such as Odf1, Odf2, and Akap4. Regarding the underlying mechanism, SUN5 regulates the process of mRNA export, and the downregulation of SUN5 results in many mRNAs trapped in the nucleus and unable to be exported to the cytoplasm for translation, resulting in the downregulation of the corresponding proteins. Therefore, we propose that SUN5 regulates the expressions of a subset of proteins involved in the process of spermiogenesis. In addition, the residual protein, which was observed in *Sun5*$^{-/-}$ mice, may be the nonfunctional SUN5 protein produced by abnormal alternative splicing.

In summary, our study demonstrated that SUN5, a nuclear membrane protein, recruits Nxf1-bound mRNP to the NE and transfers it to the NPC component Nup93, which enables successful mRNA export from the nucleus to the cytoplasm. Knockout of *Sun5* downregulates the expression of spermatogenesis-related genes, resulting in abnormal spermatogenesis. This work provides a novel specific mode of mRNA export and contributes to our understanding of the molecular mechanisms of spermatogenesis.

Supplementary Data

Supplementary data is available at *Acta Biochimica et Biophysica Sinica* online.

Acknowledgement

We thank Shuting Zhang and Jingyuan Chen (Center for Experimental Medicine, Third Xiangya Hospital of Central South University, Changsha, China) for their help in cell culture.

Funding

This work was supported by the grants from the open research fund of Hunan Provincial Key Laboratory of Regional Hereditary Birth Defects Prevention and Control (No. HPKL2023006), the Hunan Provincial Natural Science Foundation of China (No. 2023JJ30854), the Natural Science Foundation of Changsha Municipal, Hunan Province, China (No. kq2208354), and the Undergraduate and Graduate Student Independent Exploration Innovation Fund of Central South University (Nos. 1053320214303 and 1053320215869).

Conflict of Interest

The authors declare that they have no conflict of interest.

References

1. Hao SL, Ni FD, Yang WX. The dynamics and regulation of chromatin remodeling during spermiogenesis. *Gene* 2019, 706: 201–210
2. Carmody SR, Wente SR. mRNA nuclear export at a glance. *J Cell Sci* 2009, 122: 1933–1937
3. Legrand JMD, Hobbs RM. RNA processing in the male germline: mechanisms and implications for fertility. *Semin Cell Dev Biol* 2018, 79: 80–91
4. De Magistris P. The great escape: mRNA export through the nuclear pore complex. *Int J Mol Sci* 2021, 22: 11767
5. Geuens T, Bouhy D, Timmerman V. The hnRNP family: insights into their role in health and disease. *Hum Genet* 2016, 135: 851–867
6. Dreyfuss G, Kim VN, Kataoka N. Messenger-RNA-binding proteins and the messages they carry. *Nat Rev Mol Cell Biol* 2002, 3: 195–205
7. Han SP, Tang YH, Smith R. Functional diversity of the hnRNPs: past, present and perspectives. *Biochem J* 2010, 430: 379–392
8. Culjkovic-Kraljacic B, Borden KLB. Aiding and abetting cancer: mRNA export and the nuclear pore. *Trends Cell Biol* 2013, 23: 328–335
9. Xie Y, Ren Y. Mechanisms of nuclear mRNA export: a structural perspective. *Traffic* 2019, 20: 829–840
10. Katahira J, Yoneda Y. Roles of the TREX complex in nuclear export of mRNA. *RNA Biol* 2009, 6: 149–152
11. Aibara S, Katahira J, Valkov E, Stewart M. The principal mRNA nuclear export factor NXF1: NXT1 forms a symmetric binding platform that facilitates export of retroviral CTE-RNA. *Nucleic Acids Res* 2015, 43: 1883–1893
12. Schuller SK, Schuller JM, Prabu JR, Baumgärtner M, Bonneau F, Basquin J, Conti E. Structural insights into the nucleic acid remodeling mechanisms of the yeast THO-Sub2 complex. *eLife* 2020, 9: e61467
13. Heath CG, Viphakone N, Wilson SA. The role of TREX in gene expression and disease. *Biochem J* 2016, 473: 2911–2935
14. Aramburu IV, Lemke EA. Floppy but not sloppy: interaction mechanism of FG-nucleoporins and nuclear transport receptors. *Semin Cell Dev Biol* 2017, 68: 34–41
15. Beck M, Hurt E. The nuclear pore complex: understanding its function through structural insight. *Nat Rev Mol Cell Biol* 2017, 18: 73–89
16. Lin DH, Hoelz A. The structure of the nuclear pore complex (An Update). *Annu Rev Biochem* 2019, 88: 725–783
17. Li P, Noegel A A. Inner nuclear envelope protein SUN1 plays a prominent role in mammalian mRNA export. *Nucleic Acids Res* 2015, 43: 9874–9844
18. Malik P, Tabarraei A, Kehlenbach RH, Korfali N, Iwasawa R, Graham SV, Schirmer EC. Herpes simplex virus ICP27 protein directly interacts with the nuclear pore complex through Nup62, inhibiting host nucleocytoplasmic transport pathways. *J Biol Chem* 2012, 287: 12277–12292
19. Han M, Zhao M, Cheng C, Huang Y, Han S, Li W, Tu X, ***et al.*** Lamin A mutation impairs interaction with nucleoporin NUP155 and disrupts nucleocytoplasmic transport in atrial fibrillation. *Hum Mutat* 2019, 40: 310–325
20. de Bruyn Kops A, Guthrie C. Identification of the novel Nup188-brr7 allele in a screen for cold-sensitive mRNA export mutants in *Saccharomyces cerevisiae*. *G3 (Bethesda)* 2018, 8: 2991–3003
21. David-Watine B, Polymenis M. Silencing nuclear pore protein Tpr elicits a senescent-like phenotype in cancer cells. *PLoS One* 2011, 6: e22423
22. Zhang Y, Yang L, Huang L, Liu G, Nie X, Zhang X, Xing X. SUN5 interacting with nesprin3 plays an essential role in sperm head-to-tail linkage: research on sun5 gene knockout mice. *Front Cell Dev Biol* 2021, 9: 684826
23. Guo X, Xu Y, Wang Z, Wu Y, Chen J, Wang G, Lu C, ***et al.*** A linc1405/Eomes complex promotes cardiac mesoderm specification and cardiogenesis. *Cell Stem Cell* 2018, 22: 893–908.e6

24. Zhu F, Liu C, Wang F, Yang X, Zhang J, Wu H, Zhang Z, *et al.* Mutations in PMFBP1 cause acephalic spermatozoa syndrome. *Am J Hum Genet* 2018, 103: 188–199
25. Shang Y, Zhu F, Wang L, Ouyang YC, Dong MZ, Liu C, Zhao H, *et al.* Essential role for SUN5 in anchoring sperm head to the tail. *eLife* 2017, 6: e28199
26. Kim JH, Hahm B, Kim YK, Choi M, Jang SK. Protein-protein interaction among hnRNPs shuttling between nucleus and cytoplasm. *J Mol Biol* 2000, 298: 395–405
27. Forler D, Rabut G, Ciccarelli FD, Herold A, Köcher T, Niggeweg R, Bork P, *et al.* RanBP2/Nup358 provides a major binding site for NXF1-p15 dimers at the nuclear pore complex and functions in nuclear mRNA export. *Mol Cell Biol* 2004, 24: 1155–1167
28. Grund SE, Fischer T, Cabal GG, Antúnez O, Pérez-Ortín JE, Hurt E. The inner nuclear membrane protein Src1 associates with subtelomeric genes and alters their regulated gene expression. *J Cell Biol* 2008, 182: 897–910
29. Kurshakova MM, Krasnov AN, Kopytova DV, Shidlovskii YV, Nikolenko JV, Nabirochkina EN, Spehner D, *et al.* SAGA and a novel Drosophila export complex anchor efficient transcription and mRNA export to NPC. *EMBO J* 2007, 26: 4956–4965
30. Chang W, Worman HJ, Gundersen GG. Accessorizing and anchoring the LINC complex for multifunctionality. *J Cell Biol* 2015, 208: 11–22
31. Rothballer A, Kutay U. The diverse functional LINCs of the nuclear envelope to the cytoskeleton and chromatin. *Chromosoma* 2013, 122: 415–429
32. Jiang XZ, Yang MG, Huang LH, Li CQ, Xing XW. SPAG4L, a novel nuclear envelope protein involved in the meiotic stage of spermatogenesis. *DNA Cell Biol* 2011, 30: 875–882
33. Matsumoto A, Hieda M, Yokoyama Y, Nishioka Y, Yoshidome K, Tsujimoto M, Matsuura N. Global loss of a nuclear lamina component, lamin A/C, and LINC complex components SUN 1, SUN 2, and nesprin-2 in breast cancer. *Cancer Med* 2015, 4: 1547–1557
34. Liu L, Li SW, Yuan W, Tang J, Sang Y. Downregulation of SUN2 promotes metastasis of colon cancer by activating BDNF/TrkB signalling by interacting with SIRT1. *J Pathol* 2021, 254: 531–542
35. Knaup KX, Monti J, Hackenbeck T, Jobst-Schwan T, Klanke B, Schietke RE, Wacker I, *et al.* Hypoxia regulates the sperm associated antigen 4 (SPAG4) via HIF, which is expressed in renal clear cell carcinoma and promotes migration and invasion *in vitro*. *Mol Carcinog* 2014, 53: 970–978
36. Ji Y, Jiang J, Huang L, Feng W, Zhang Z, Jin L, Xing X. Sperm-associated antigen 4 (SPAG4) as a new cancer marker interacts with Nesprin3 to regulate cell migration in lung carcinoma. *Oncol Rep* 2018, 40: 783–792
37. Liu T, Yu J, Ge C, Zhao F, Chen J, Miao C, Jin W, *et al.* Sperm associated antigen 4 promotes SREBP1-mediated de novo lipogenesis via interaction with lamin A/C and contributes to tumor progression in hepatocellular carcinoma. *Cancer Lett* 2022, 536: 215642
38. Song X, Li R, Liu G, Huang L, Li P, Feng W, Gao Q, *et al.* Nuclear membrane protein SUN5 is highly expressed and promotes proliferation and migration in colorectal cancer by regulating the ERK pathway. *Cancers (Basel)* 2022, 14: 5368
39. Ding X, Xu R, Yu J, Xu T, Zhuang Y, Han M. SUN1 Is required for telomere attachment to nuclear envelope and gametogenesis in mice. *Dev Cell* 2007, 12: 863–872
40. Link J, Leubner M, Schmitt J, Göb E, Benavente R, Jeang KT, Xu R, *et al.* Analysis of meiosis in SUN1 deficient mice reveals a distinct role of SUN2 in mammalian meiotic LINC complex formation and function. *PLoS Genet* 2014, 10: e1004099
41. Xiang M, Wang Y, Wang K, Kong S, Lu M, Zhang J, Duan Z, *et al.* Novel mutation and deletion in SUN5 cause male infertility with acephalic spermatozoa syndrome. *Reprod Sci* 2022, 29: 646–651
42. Li X, Wu Y, Huang L, Yang L, Xing X. SPAG4L/SPAG4L interacts with Nesprin2 to participate in the meiosis of spermatogenesis. *Acta Biochim Biophys Sin* 2019, 51: 669–676
43. Xu H, Guo J, Wu W, Han Q, Huang Y, Wang Y, Li C, *et al.* Deletion of hnrnpk gene causes infertility in male mice by disrupting spermatogenesis. *Cells* 2022, 11: 1277